

# Transfer Learning Based Detection for Intelligent Reflecting Surface Aided Communications

Saud Khan, Salman Durrani, and Xiangyun Zhou

School of Engineering, The Australian National University, Canberra, 2601, Australia.

Email: {saud.khan, salman.durrani, xiangyun.zhou}@anu.edu.au

**Abstract**—This work investigates the data detection problem in an Intelligent Reflecting Surface (IRS) aided downlink communication between a multi-antenna access point (AP) and multiple user equipments (UEs). We utilise a deep learning-based approach, with a maximum likelihood detection (MLD)-based loss function, thereby bypassing the resource-consuming channel training and estimation requirement for detection. The proposed detection framework first trains a base deep neural network (DNN) offline with the simulated samples of the channel coefficients and IRS phase shifts in the IRS-assisted communications scenario. To deal with the significant challenge of the channel getting outdated, domain adaptation under the transfer learning paradigm is leveraged, i.e., the initial layers of the DNN are frozen, and the remaining layers are retrained on a smaller number of the received signal samples online to account for the channel mismatch. Our results show that the proposed detector achieves BER results close to the lower bound and outperforms conventional benchmark techniques, with relatively lower complexity.

**Index Terms**—Intelligent Reflecting Surface, deep learning, transfer learning, detection.

## I. INTRODUCTION

Recent advances in Intelligent Reflecting Surfaces (IRS) have drawn significant attention due to their ability to control the propagation environment, achieve a power gain with low-cost hardware, and ease of their practical deployment against walls or ceilings [1], [2]. These surfaces consist of small, passive reconfigurable elements that reflect the incident signal towards the user equipments (UEs) with a controllable phase shift. Since the UEs receives a reflected signal, estimating the channels and IRS phase shift matrix for data detection at the UE is a significant research problem.

In order to fully reap the benefits provided by the IRS, an inherent practical implementation issue is that the proper data detection critically depends on accurate channel state information (CSI). Since the passive IRS elements lack baseband processing capabilities, they are incapable of transmitting and receiving pilot signals. Thus, the conventional approach of pilot-aided channel estimation cannot be applied at the UE in IRS-aided communication systems [3]–[6]. Assuming perfect CSI availability, existing work in the literature has focused on beamforming and IRS phase shift matrix optimization using semi-definite relaxation (SDR) methods [7], [8]. In these early works, the problem was formulated to minimise the total transmit power by jointly optimizing the transmit beamforming and IRS phase shifts, subject to the signal to-

interference-plus-noise ratio (SINR) and discrete phase-shift constraints. However, these schemes require the knowledge of perfect CSI for detection, resulting in massive overhead for channel training and estimation [4]. Recently, some works have addressed channel estimation in IRS-aided multi-user systems [5], [6], [9]. However, the focus is on using the estimated CSI to design the beamforming and IRS phase shift matrix in order to maximize the system performance and data detection at UEs is not addressed.

Recent advances in deep learning (DL) have made it possible to obtain solutions to the detection problem using data-driven techniques [10]–[14]. This avoids the need for resource-consuming channel training and estimation altogether, and is an attractive solution for IRS-aided communications. In this regard, the compressed sensing framework in [10] assumes IRS has active elements, the twin convolutional neural networks based approach in [11] has computational complexity which grows exponentially for large scale systems. Similarly, the deep reinforcement learning (DRL) based approach in [12] requires the complete communication framework as a training ground. Therefore, its application for detection comes at the cost of requiring a much higher computational complexity at the training and deployment stage. Compared to DRL, DL based models provide higher flexibility since they do not involve the AP and IRS for detection [13]. However, DL based techniques inherently fail to perform well in a mismatch scenario, where the actual channels are different from the channels used to train the model [14]. In this regard, domain adaptation under the transfer learning paradigm [15], [16] has tremendous potential to be applied to improve the detection performance under a mismatch scenario.

The main contributions of this work are:

- We propose a solution to the data detection problem in an IRS aided downlink communication between a multi-antenna access point (AP) and multiple UEs using a deep transfer learning framework. What distinguishes this work from prior techniques in the literature is that we use the transfer learning paradigm to quickly update the deep neural network (DNN) using a smaller number of the received signal samples. This significantly reduces the time and computational complexity requirements to retrain the DNN.
- Our results show that the proposed method achieves average bit error rate (BER) results close to the lower

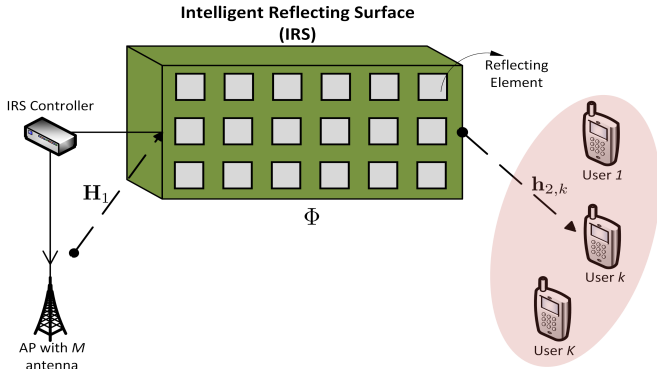


Fig. 1: Illustration of IRS-aided multi-user downlink system.

bound and outperforms conventional benchmark techniques, such as weighted minimum mean square error (WMMSE) and regularised zero-forcing (ZF), in terms of the average BER.

*Notations:* The following notations are used in this paper. Lower and upper case boldface letters are used for vectors and matrices, respectively. The Hermitian transpose of a matrix  $\mathbf{A}$  is  $\mathbf{A}^H$ . The estimated value of  $a$  is denoted by  $\hat{a}$ . The Euclidian norm is denoted by  $\|\cdot\|$ .  $\mathbb{C}^{x \times y}$  denotes the space of  $x \times y$  complex-valued matrices.  $\text{tr}\{\cdot\}$  denotes the trace operation,  $\text{diag}(\cdot)$  denotes the diagonal operation, whereas  $\mathbb{E}(\cdot)$  denotes expectation operator.  $\Re(\cdot)$  and  $\Im(\cdot)$  denote the real and imaginary parts of a complex number respectively. The gradient differential operator is denoted by  $\nabla$ .

## II. SYSTEM MODEL

We consider a multi-input single-output (MISO) downlink system, comprising of an AP, an IRS, and  $K$  UEs, as shown in Fig. 1. We assume that the direct communication path between AP and UEs is blocked, and the IRS is deployed to reflect the AP's signal towards the UEs. The AP is equipped with  $M$  antenna elements, while all UEs have a single antenna. The IRS is composed of  $N$  passive elements controlled using an IRS controller.

We consider the quasi-static frequency flat-fading channels and use maximum-ratio transmission as the optimal beamforming strategy at the AP, as in [8]. The beamforming vector at the  $k^{\text{th}}$  UE is denoted as  $\mathbf{v}_k \in \mathbb{C}^{M \times 1}$ . Thus, the complex modulated transmitted signal at the AP can be expressed as  $\mathbf{x} = \sum_{j=1}^K \mathbf{v}_j s_j$ , where  $s_j$  denotes the transmitted data for user  $j$ . Furthermore,  $s_j$  are independent random variables drawn from standard symmetric  $M$ -ary discrete constellation set. Additionally, the total transmit power allowed at the AP follows the constraint  $\mathbb{E}\{\text{tr}\{\mathbf{V}\mathbf{x}(\mathbf{V}\mathbf{x})^H\}\} \leq P_{\max}$ , where  $\mathbf{V} \triangleq [\mathbf{v}_1, \mathbf{v}_2, \dots, \mathbf{v}_K] \in \mathbb{C}^{M \times K}$ , and  $P_{\max}$  is the maximum transmit power at the AP [12].

The signal received at the  $k^{\text{th}}$  UE from the AP-IRS-UE path

is expressed as [12],

$$y_k = \underbrace{(\mathbf{h}_{2,k}^H \Phi \mathbf{H}_1) \mathbf{v}_k s_k}_{\text{desired signal}} + \underbrace{\sum_{j \neq k}^K (\mathbf{h}_{2,k}^H \Phi \mathbf{H}_1) \mathbf{v}_j s_j}_{\text{co-channel interference}} + w_k, \quad (1)$$

where  $k = 1, 2, \dots, K$ , is the UE index.  $\mathbf{H}_1 \in \mathbb{C}^{N \times M}$  denotes the channel matrix from the AP to IRS,  $\mathbf{h}_{2,k}^H \in \mathbb{C}^{1 \times N}$  denotes the channel vector from the IRS to  $k^{\text{th}}$  UE.  $\Phi = \text{diag}[x_1 e^{j\theta_1}, \dots, x_N e^{j\theta_N}] \in \mathbb{C}^{N \times N}$  is a diagonal matrix representing the adjustable phase angle induced by the IRS where  $x_i \in [0, 1]$  and  $\theta_i \in [0, 2\pi)$  represent amplitude reflection factor and the phase shift coefficient for the  $i^{\text{th}}$  IRS element. Finally,  $w_k$  denotes the complex additive white Gaussian noise (AWGN) with zero mean and variance  $\sigma_k^2$ .

In this work, we employ random phase shifting design for the IRS [17]. This design avoids the system overhead caused by acquiring global CSI at the AP. It is also more practical than coherent phase shifting design, where the phase shift of each reflecting element is matched to the phases of its incoming and outgoing fading channels, because of the finite resolution of practical phase shifters [8], [17]–[19]. Our results in Section IV will show that acceptable BER is achieved with random discrete phase shifting design.<sup>1</sup>

In this work, we are interested in the individual detection of data streams at the UEs, treating co-channel interference as noise. For a phase shift matrix  $\Phi$ , the optimal detection technique for the IRS-aided communication system is the maximum likelihood detection (MLD) [20]. This is because MLD uses an exhaustive search to evaluate all possible combinations of transmitted signals. The evaluation of received symbols at the  $k^{\text{th}}$  UE is determined using the Euclidean minimum-distance criterion as,

$$\hat{\mathbf{x}} = \arg \min_{\mathbf{x}_k} \left\| \mathbf{y}_k - (\mathbf{h}_{2,k}^H \Phi \mathbf{H}_1) \mathbf{x}_k \right\|^2, \quad (2)$$

The UE needs to accurately estimate the channels  $\mathbf{H}_1$ ,  $\mathbf{h}_{2,k}^H$ , and the phase shift matrix  $\Phi$ , in order to decode the received symbols correctly.

In this paper, rather than trying to solve the challenging detection problem using classical pilot based signaling or computationally exhaustive DRL, we propose a solution in the context of DL with transfer learning. In our case, the objective of the DNN is to map the relationship between the received signal, which is impaired by the AP-IRS and IRS-UE channels and the phase shift matrix of the IRS, and the downlink transmitted signal, without any dependence on the AP.

## III. PROPOSED DEEP LEARNING DETECTOR

This section details the proposed DL detector for the IRS assisted communication scenario in Section I. First, details of the base training of the DNN are presented. Next, the transfer learning paradigm is discussed. The proposed detector is illustrated in Fig. 2.

<sup>1</sup>Note that phase shifting design to enhance the detection is possible but is outside the scope of this work.

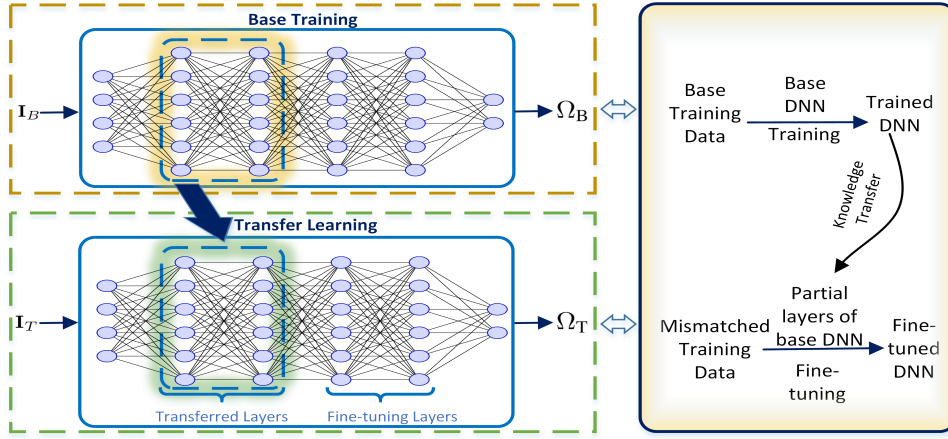


Fig. 2: The proposed deep transfer learning based detector.

### A. Base Training of DNN

A DNN consists of  $\ell$  fully-connected layers with multiple neurons in every layer. The output of the network  $\Omega_B$  is a cascade of the nonlinear transformation of input data  $\mathbf{I}_B$ , split into batch size  $B$ , through all the previous layers, which is carried out iteratively. The output of the network can be expressed as [21],

$$\Omega_B = f_{\Theta_B}(\mathbf{I}_B) = f^{(\ell-1)}(f^{(\ell-2)}(\dots f^{(1)}(\mathbf{I}_B))) \quad (3)$$

where  $\Theta_B$  represents the weights and biases of the DNN and for each layer,

$$f_i = \sigma(w_i \mathbf{I}_B + b_i) \quad (4)$$

where each layer has at its output an activation function  $\sigma(\cdot)$ , and corresponding weights  $w_i$ . An additional bias term  $b_i$  is also added to balance the sparse weight balancing during training.

The purpose of DNN is to find the mapping function between input and output, based on the training data, and therefore, approximate the next samples based on the universal approximation theorem [22]. The training process for the DNN is carried out by a dataset comprising of input-output pairs  $\{y, \Omega\}$ . The input-output vectors contain complex numbers, which are split into real and imaginary entries, such that  $\Omega = [\Re(\mathbf{x}), \Im(\mathbf{x})]^T$ . Based on this, we utilise sequence-to-sequence regression for training and testing phases, where the pairs are stacked into categorical arrays of dimension  $L \times 1$  as input to the DNN, where  $L$  is the number of transmit signal-to-noise (SNR) ratios at which the signal is transmitted for training. Based on (2), the loss function for the proposed DL model is formulated as,

$$\mathcal{L}(\Theta) = \frac{1}{N} \sum_n \|\hat{\Omega}(n) - \Omega(n)\|_2^2 + \lambda \sum_n \Theta_n^2, \quad (5)$$

where the DNN derives the mapping function obtained from the received signal over  $n$  iterations. This process yields a generic formulation for the estimation of the channels and phase shift matrix in the hidden layers of DNN at the  $n^{\text{th}}$

iteration. Moreover,  $\Theta$  is updated at every iteration using the Adam optimiser as,

$$\Theta_{\ell+1} = \Theta_{\ell} - \frac{\eta m_{\ell}}{\sqrt{v_{\ell} + \epsilon}}, \quad (6)$$

where  $\eta$  is the learning rate with which the optimiser defines the learning step size, and  $\epsilon$  is a smoothing term that prevents division by zero. Furthermore,  $m_{\ell}$  and  $v_{\ell}$  are estimates of the mean and uncentered variance of the gradients, respectively, defined as,

$$\begin{aligned} m_{\ell} &= \delta_1 m_{\ell-1} + (1 - \delta_1) \nabla \mathcal{L}(\Theta_{\ell}) \\ v_{\ell} &= \delta_2 v_{\ell-1} + (1 - \delta_2) \nabla [\mathcal{L}(\Theta_{\ell})]^2, \end{aligned} \quad (7)$$

where  $\delta_1$  and  $\delta_2$  are the decay rates of the moving average. If the gradients in (7) are similar over many iterations, the moving average helps the gradients to gain momentum in a specific direction. Conversely, if the gradients are highly noisy because of sparse training data, then the gradient's moving average is smaller, so the parameter updates are also smaller. This helps in controlling the step size of the optimiser in order to correctly identify the global optimum solution of the training set, and prevents the network from looping in a local solution.

### B. Transfer Learning of DNN

Transfer learning, which focuses on transferring the knowledge across domains, is a promising machine learning methodology to improve the learning accuracy with fewer labelled data [23]. Domain adaptation refers to the process of improving the performance of the learning task by using a DNN to discover and transfer latent knowledge from the source domain to target domain. Note that in this paper, the source domain data and the target domain data arise from the training sets of offline learning and transfer learning, respectively [16], [23]. In this regard, the transfer learning approach allows the designed detector to adapt itself properly to different channel environments for improving the system performance.

The DNN described in Section II-A is not well suited on its own to converge towards the solution in (2). This

---

**Algorithm 1** Deep Transfer Learning Based Detection

---

**Initialise:**  $\Theta_B, \Theta_T$  with random weights, the learning rate  $\eta$ , the batch size  $B$ , validation error threshold set to  $n_B$  for base training and  $n_T$  for transfer learning.

1: **Base Training:**2: **Input:** Training patches  $\mathbf{I}_B$ 3: Produce  $\mathbf{I}_B$  with simulated CSI  $\mathbf{h}_{2,k}^H, \mathbf{H}_1$  and phase shift matrix  $\Phi$ , according to (1).4: **while** ( $n_B \leq \mathcal{L}$ ) Split  $\mathbf{I}_B$  into  $B$  mini-batches and set learning rate to  $\eta$ 

5: Train the DNN by minimizing the loss function according to (5).

6: Update  $\mathcal{L}(\Theta)$  according to (6) and (7).7: **end while**8: **Output:** Base DNN,  $\Omega_B$ 

9:

10: **Transfer Learning:**11: **Input:** Training patches  $\mathbf{I}_T$ , Base DNN12: Obtain  $\mathbf{I}_T$  with mismatched CSI  $\mathbf{h}_{2,k}^H, \mathbf{H}_1$  and phase shift matrix  $\Phi$ 13: Freeze the weights  $\Theta_B$  for initial layers of the base DNN, such that  $f_{\Theta_B}^{TL}(\mathbf{I}_B)$ 14: **while** ( $n_T \leq \mathcal{L}$ ) Split  $\mathbf{I}_T$  into  $B$  mini-batches and set learning rate to  $\eta$ 15: Fine tune the DNN by minimizing the loss function according to (5), such that  $f_{\Theta_T}(\mathbf{I}_T) = f_{\Theta_T}^{FL}(f_{\Theta_B}^{TL}(\mathbf{I}_B))$ 16: Update  $\mathcal{L}(\Theta)$  according to (6) and (7).17: **end while**18: **Output:** Transfer learned DNN,  $\Omega_T$ 

---

is because during base training, the DNN is initialised with random weights and trained over  $n$  iterations in offline mode, until the network converges. However, as new channel samples are received, the DNN gets outdated, and requires retraining, which is a resource-consuming task.

In this work, we overcome this inherent limitation of the DNN by utilising domain adaptation under the transfer learning paradigm, as illustrated in Fig. 2. Domain adaptation aims to improve a trained DNN for a learning task by quickly transferring latent knowledge from new samples to the already trained DNN. This essentially means that partial layers of the pre-trained DNN are frozen<sup>2</sup>. Only the remaining layers are fine-tuned to adjust the DNN to the current channel coefficients for performance improvement. Based on this, the DNN with transfer learning capability can be expressed as [23],

$$\Omega_T = f_{\Theta_T}(\mathbf{I}_T) = f_{\Theta_T}^{FL}(f_{\Theta_B}^{TL}(\mathbf{I}_B)) \quad (8)$$

where  $f_{\Theta_T}(\cdot)$  is the expression for the optimised DNN through transfer learning with updated hyper-parameters  $\Theta_T$ .  $f_{\Theta_T}^{FL}(\cdot)$  represents the fine-tuning layers of the DNN, and  $f_{\Theta_B}^{TL}(\cdot)$  represents the layers in the frozen state, with its corresponding

<sup>2</sup>Layer freezing means that the layer weights of a pre-trained DNN keep unchanged during training in a subsequent task, i.e., they remain frozen.

TABLE I: Description of hyper-parameters used for the proposed deep transfer learning based detection framework.

Parameter	Description	Value
$\eta$	Learning rate for training the DL network	0.01
$n_B$	Number of training iterations for base training	1000
$n_T$	Number of training iterations for transfer learning	100
$B$	Batch size for split training and testing sets	32
$\epsilon$	Smoothing term to prevent division by zero for Adam	$10^{-8}$
$\delta_1, \delta_2$	Decay rates of the moving average for Adam	$\delta_1 = 0.9,$ $\delta_2 = 0.99$
$\mathbf{I}_B$	The number of training samples used for base training	$L \times 10^5$
$\mathbf{I}_T$	The number of training samples used for retraining of base network in a mismatch scenario	$L \times 10^3$
Regularisation	Ridge regression, $\lambda$ , and dropout layer probability, $p$ , to address over-fitting	$\lambda = 10^{-4},$ $p = 0.3$
Validation split	Splitting ratio of training set for validation of DL network	20%
Validation patience	Stoppage threshold for linear validation curve during training	5

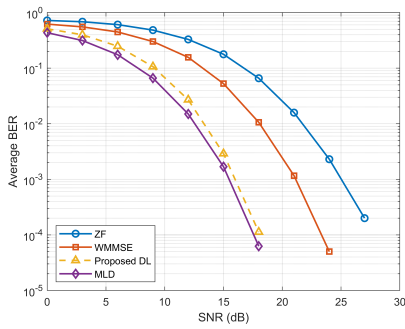
trained hyper-parameters  $\Theta_B^*$ . Since the objective is to fine-tune the already trained network, the complete set of received signal samples as a training set is not required, and only a smaller set of samples is needed. The proposed deep transfer learning based detection algorithm is detailed in Algorithm 1 and the description of the hyper-parameters is given in Table I.

*Remark 1:* The received signal reflected by the IRS experiences fading through the channels, and an additional phase shift is added to it by the IRS. Consequently, the received signal at the UE contains important phase and channel coefficients mapping information. DNNs can learn this mapping based on the received signal itself, instead of relying explicitly on pilot signaling for channel and phase angle estimation. This essentially makes the DNN a decentralised solution, and does not require any CSI for detection. Other (centralised) conventional techniques, such as WMMSE [24] and ZF [25], require full CSI for detection. Since the DNN's loss function in (6) is derived from the MLD, the DNN will not outperform it. Rather, the DNN will at best perform in-par with the MLD whilst having lower complexity and better performance than conventional techniques.

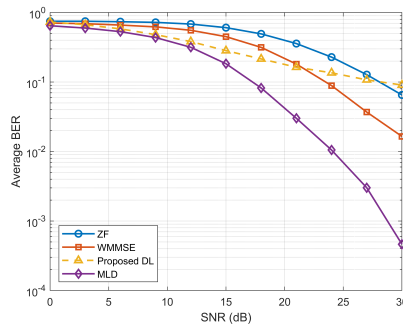
## IV. RESULTS

In this section, we provide results to demonstrate the performance of the proposed detection framework. We consider a three-dimensional (3D) coordinate system with the AP and the IRS in the  $x$ -axis and  $x-z$  axis, respectively. For simplicity, the AP is located at  $(0, 0, 0)$  m and the IRS is located at  $(2, d_r, 2)$  m, where  $d_r > 0$  is the distance between them. The UEs are randomly placed within a distance  $d_u$  from the IRS, such that  $1 \leq d_u \leq 10$  m.

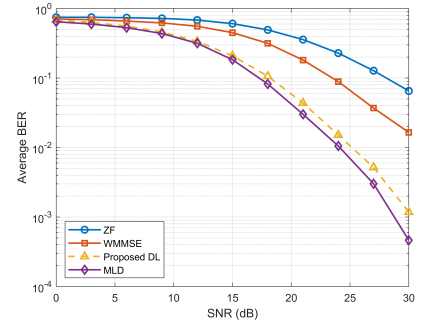
Following [26], the Rayleigh fading channels are generated as follows:  $\tilde{\mathbf{H}}_1 = L_r \mathbf{H}_1$  and  $\tilde{\mathbf{h}}_{2,k}^H = L_u \mathbf{h}_{2,k}^H$  where  $\mathbf{H}_1$  and  $\mathbf{h}_{2,k}^H$  have independent and identically  $\mathcal{CN}(0, 1)$  elements. The pathloss for the IRS-UE link is set as  $L_u = \sqrt{\beta_0(d_u/d_0)^{-\alpha}}$



(a) BER under matched CSI.



(b) BER under mismatched CSI.



(c) BER under mismatched CSI - after transfer learning.

Fig. 3: Average BER results under different CSI conditions.

where  $\alpha = 3.75$  is the pathloss exponent,  $d_0 = 1$  m is the reference distance,  $d_u$  is the distance between IRS and UE, and  $\beta_0 = -20.4$  dB is the reference pathloss. Similarly, the pathloss for the AP-IRS link is set as  $L_r = \frac{N d_{ar}^2}{4\pi d_r}$  where  $d_{ar} = 0.25$  m is the area of one IRS element and  $d_r = 45$  m is the distance between the AP and IRS.

In this work, our goal is not to optimize the performance of a given IRS-aided communication system by designing a phase shift matrix. Hence, we consider random reflection pattern for the IRS, i.e., phase shifts are uniformly distributed within  $[0, 2\pi)$  and reflection amplitudes are uniformly distributed within  $[0, 1]$  [17]. Unless specified otherwise, the main system parameters are as follows:  $M = 8$ ,  $N = 64$ ,  $K = 8$ ,  $P_{\max} = 30$  dB,  $\sigma_k^2 = -80$  dBm. We use QPSK as the modulation scheme. We average all results over 1000 independent realisations.

In the proposed deep transfer learning based framework, the DNN is composed of four fully-connected dense layers, with the number of neurons as 500, 250, 100 and 50, respectively. Every layer is preceded by a tangent-hyperbolic activation function to facilitate the modulated data's real and imaginary parts. The final layer is facilitated with an additional dropout layer whereas the training data is shuffled at every iteration to facilitate the network with over-fitting resistance. During base training, the network is trained on the training patches  $\mathbf{I}_B$ , and then deployed for detection. During mismatch, the weights of the first two layers of the network are frozen, and the remaining layers are re-trained with the new channel samples  $\mathbf{I}_T$ . The values of the hyper-parameters used for training, based on test and trial method, are shown in Table I.

#### A. Performance metrics

We evaluate the performance of the base DNN with matched CSI, the base DNN with mismatched CSI, and the base DNN with mismatched CSI after domain adaptation using transfer learning using the average BER of the UEs. In the context of the DNN, the matched CSI means that the channels are the same as during base training and the mismatched scenario means that the channels are different from the ones during base training. The average BER is calculated by taking the mean of BER of all users. The MLD is used as the optimal lower

bound. Furthermore, we plot the performance of conventional WMMSE [24] and regularised ZF [25] for benchmarking, which require full CSI for detection.

#### B. Comparison with benchmarks showing the advantage of transfer learning

Fig. 3(a) plots the average BER result under the cases of matched CSI, Fig. 3(b) under mismatched CSI, and Fig. 3(c) under mismatched CSI after transfer learning. Fig. 3(a) shows that under matched CSI, the average BER achieved by the base DNN is quite close to the optimal MLD and outperforms both the benchmarks. This is in line with the performance, as expected in Remark 1.

Since the wireless channels can vary over time, we consider a harsh mismatched scenario. For this, we increase the IRS-UE distance to  $10 \leq d_u \leq 15$  m and set  $\alpha = 5$ . Fig. 3(b) show that under a mismatched CSI scenario, the average BER of the base DNN degrades significantly. This is because of the DNN's inability to correctly capture and classify the changed channel conditions. To tackle this, we use the domain adaptation ability of transfer learning as proposed in Algorithm 1. Thus, the final two layers of the base DNN are retrained with the mismatch training data, while the rest of the network layers/weights are kept in a frozen state. This results in the DNN keeping the initial learned weights intact while updating the latter according to the new data. Figs. 3(c) show that after domain adaptation, the average BER of the system is again close to MLD and the proposed detection algorithm outperforms the benchmarks in terms of average BER.

#### C. Convergence and complexity of proposed algorithm

Fig. 4 shows the training performance of the proposed deep learning detector in terms of root mean square error (RMSE). The RMSE is defined as the square root of the loss function in (6). We can see that both the training and validation curves converge in a small number of iterations ( $< 30$ ). The proposed detection scheme also has much lower complexity than other techniques in the literature, as listed in Table II using the Big- $\mathcal{O}$  notation. This further demonstrates the benefits of the proposed solution.

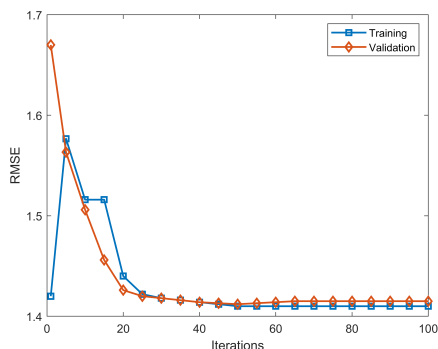


Fig. 4: Training of the proposed detection framework.

## V. CONCLUSION

This work proposed a solution to the detection problem in an IRS-aided multi-user downlink MISO wireless communication system. A deep transfer learning-based detection framework was proposed to solve this problem, bypassing the need for resource-consuming channel training and estimation at the UEs. The results showed that the proposed detector can efficiently improve the performance in a mismatched scenario, where the actual channels are different from the channels used to train the model.

## VI. ACKNOWLEDGEMENT

This research was undertaken with the assistance of resources and services from the National Computational Infrastructure (NCI), which is supported by the Australian Government.

## REFERENCES

- [1] M. Di Renzo, M. Debbah, D.-T. Phan-Huy *et al.*, “Smart radio environments empowered by reconfigurable AI meta-surfaces: An idea whose time has come,” *J Wireless Com Network.*, vol. 2019, no. 1, pp. 1–20, May. 2019.
- [2] S. Gong, X. Lu, D. T. Hoang, D. Niyato, L. Shu, D. I. Kim, and Y.-C. Liang, “Towards smart wireless communications via intelligent reflecting surfaces: A contemporary survey,” *IEEE Commun. Surveys Tuts.*, vol. 22, no. 4, pp. 2283–2314, Jun. 2020.
- [3] Q. Wu, S. Zhang, B. Zheng, C. You, and R. Zhang, “Intelligent reflecting surface aided wireless communications: A tutorial,” *IEEE Trans. Commun.*, Jan. 2021 (accepted, to appear).
- [4] B. Zheng, C. You, and R. Zhang, “Intelligent reflecting surface assisted multi-user OFDMA: Channel estimation and training design,” *IEEE Trans. Wireless Commun.*, vol. 19, no. 12, pp. 8315–8329, Sep. 2020.
- [5] Q.-U.-A. Nadeem, H. Alwazani, A. Kammoun, A. Chaaban, M. Debbah, and M.-S. Alouini, “Intelligent reflecting surface assisted multi-user MISO communication: Channel estimation and beamforming design,” *arXiv preprint arXiv:2005.01301*, May. 2020.
- [6] C. Jia, J. Cheng, H. Gao, and W. Xu, “High-resolution channel estimation for intelligent reflecting surface-assisted MmWave communications,” in *Proc. IEEE PIMRC.*, Oct. 2020, pp. 1–6.
- [7] Q. Wu and R. Zhang, “Intelligent reflecting surface enhanced wireless network via joint active and passive beamforming,” *IEEE Trans. Wireless Commun.*, vol. 18, no. 11, pp. 5394–5409, Nov. 2019.
- [8] Q. Wu and R. Zhang, “Beamforming optimization for intelligent reflecting surface with discrete phase shifts,” in *Proc. IEEE ICASSP*, May. 2019, pp. 7830–7833.
- [9] C. Psomas, I. Chrysovergis, and I. Krikidis, “Random rotation-based low-complexity schemes for intelligent reflecting surfaces,” in *Proc. IEEE PIMRC.*, Oct. 2020, pp. 1–6.

TABLE II: Complexity comparison with benchmarks.

Technique	Complexity
MLD	$\mathcal{O}(2^K)$
WMMSE in [24]	$\mathcal{O}(K^2M + K^2M^2 + K^2M^3 + K)$
SDR in [7]	$\mathcal{O}(N + 1)^6$
DRL in [12]	$\mathcal{O}(2K + 2K^2 + 2N + 2MK + 2NM + 2KN)$
Proposed DL	$\mathcal{O}(2K + 2NM + 2KN)$

- [10] A. Taha, M. Alrabeiah, and A. Alkhateeb, “Enabling large intelligent surfaces with compressive sensing and deep learning,” *arXiv preprint arXiv:1904.10136*, Apr. 2019.
- [11] A. M. Elbir, A. Papazafeiropoulos, P. Kourtessis, and S. Chatzinotas, “Deep channel learning for large intelligent surfaces aided mm-wave massive MIMO systems,” *IEEE Wireless Commun. Lett.*, vol. 9, no. 9, pp. 1447–1451, May. 2020.
- [12] C. Huang, R. Mo, and C. Yuen, “Reconfigurable intelligent surface assisted multiuser MISO systems exploiting deep reinforcement learning,” *IEEE J. Sel. Areas Commun.*, vol. 38, no. 8, pp. 1839–1850, Jun. 2020.
- [13] S. Khan, K. S. Khan, N. Haider, and S. Y. Shin, “Deep-learning-aided detection for reconfigurable intelligent surfaces,” *arXiv preprint arXiv:1910.09136v2*, Oct. 2019.
- [14] S. Khan and S. Y. Shin, “Deep learning aided transmit power estimation in mobile communication system,” *IEEE Commun. Lett.*, vol. 23, no. 8, pp. 1405–1408, Jun. 2019.
- [15] Y. Yuan, G. Zheng, K.-K. Wong, B. Ottersten, and Z.-Q. Luo, “Transfer learning and meta learning based fast downlink beamforming adaptation,” *IEEE Trans. Wireless Commun.*, vol. 20, no. 3, pp. 1742–1755, 2021.
- [16] F. Zhuang, Z. Qi, K. Duan, D. Xi, Y. Zhu, H. Zhu, H. Xiong, and Q. He, “A comprehensive survey on transfer learning,” *Proc. IEEE*, vol. 109, no. 1, pp. 43–76, Jul. 2020.
- [17] Z. Ding, R. Schober, and H. V. Poor, “On the impact of phase shifting designs on IRS-NOMA,” *IEEE Wireless Commun. Lett.*, vol. 9, no. 10, pp. 1596–1600, Apr. 2020.
- [18] C. You, B. Zheng, and R. Zhang, “Channel estimation and passive beamforming for intelligent reflecting surface: Discrete phase shift and progressive refinement,” *IEEE J. Sel. Areas Commun.*, vol. 38, no. 11, pp. 2604–2620, Jul. 2020.
- [19] Z. Ji, P. L. Yeoh, G. Chen, C. Pan, Y. Zhang, Z. He, H. Yin, and Y. Li, “Random shifting intelligent reflecting surface for otp encrypted data transmission,” *IEEE Wireless Communications Letters*, Feb. 2021 (accepted, to appear).
- [20] E. Basar, “Reconfigurable intelligent surface-based index modulation: A new beyond MIMO paradigm for 6G,” *IEEE Trans. Commun.*, vol. 68, no. 5, pp. 3187–3196, Feb. 2020.
- [21] H. Ye, G. Y. Li, and B.-H. Juang, “Power of deep learning for channel estimation and signal detection in OFDM systems,” *IEEE Wireless Commun. Lett.*, vol. 7, no. 1, pp. 114–117, Sep. 2017.
- [22] I. Goodfellow, Y. Bengio, and A. Courville, *Deep learning*. MIT press, 2016.
- [23] C. Liu, Z. Wei, D. W. K. Ng, J. Yuan, and Y. C. Liang, “Deep transfer learning for signal detection in ambient backscatter communications,” *IEEE Trans. Wireless Commun.*, vol. 20, no. 3, pp. 1624–1638, Nov. 2021.
- [24] Q. Shi, M. Razaviyayn, Z.-Q. Luo, and C. He, “An iteratively weighted MMSE approach to distributed sum-utility maximization for a MIMO interfering broadcast channel,” *IEEE Trans. Signal Process.*, vol. 59, no. 9, pp. 4331–4340, Apr. 2011.
- [25] Z. Wang and W. Chen, “Regularized zero-forcing for multi-antenna broadcast channels with user selection,” *IEEE Wireless Commun. Lett.*, vol. 1, no. 2, pp. 129–132, Apr. 2012.
- [26] Ö. Özdoğan, E. Björnson, and E. G. Larsson, “Intelligent reflecting surfaces: Physics, propagation, and pathloss modeling,” *IEEE Wireless Commun. Lett.*, vol. 9, no. 5, pp. 581–585, Dec. 2019.